ACS Synthetic Biology
Research Article
Cite This: ACS Synth. Biol. 2018, 7, 2457−2467
pubs.acs.org/synthbio

Engineered Biosensors from Dimeric Ligand-Binding Domains

Benjamin W. Jester,[†,‡,⊥] Christine E. Tinberg,[§,¶] Matthew S. Rich,[‡,#] David Baker,[†,§] and Stanley Fields*[,†,‡,∥]

[†]Howard Hughes Medical Institute, University of Washington, Seattle, Washington 98195, United States
[‡]Department of Genome Sciences, University of Washington, Seattle, Washington 98195, United States
[§]Department of Biochemistry, University of Washington, Seattle, Washington 98195, United States
[∥]Department of Medicine, University of Washington, Seattle, Washington 98195, United States

Supporting Information

ABSTRACT: Biosensors are important components of many synthetic biology and metabolic engineering applications. Here, we report a second generation of *Saccharomyces cerevisiae* digoxigenin and progesterone biosensors based on destabilized dimeric ligand-binding domains that undergo ligand-induced stabilization. The biosensors, comprising one ligand-binding domain monomer fused to a DNA-binding domain and another fused to a transcriptional activation domain, activate reporter gene expression in response to steroid binding and receptor dimerization. The introduction of a destabilizing mutation to the dimer interface increased biosensor dynamic range by an order of magnitude. Computational redesign of the dimer interface and functional selections were used to create heterodimeric pairs with further improved dynamic range. A heterodimeric biosensor built from the digoxigenin and progesterone ligand-binding domains functioned as a synthetic "AND"-gate, with 20-fold stronger response to the two ligands in combination than to either one alone. We also identified mutations that increase the sensitivity or selectivity of the biosensors to chemically similar ligands. These dimerizing biosensors provide additional flexibility for the construction of logic gates and other applications.

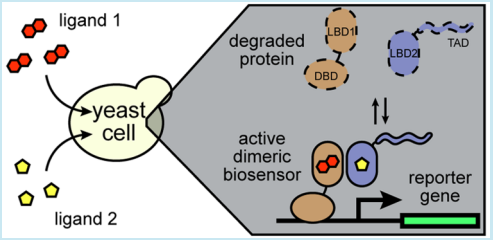

KEYWORDS: *biosensor, protein engineering, ligand-binding domain, logic gate, transcription factor, directed evolution, next generation sequencing*

Biosensors that detect small molecules can facilitate the engineering of microbial strains that synthesize useful bioproducts,[1,2] especially when combined with recent technologies that can generate hundreds of thousands of combinations of variant enzymes and promoters.[3,4] Such biosensors allow the identification of those strains producing the highest concentrations of desired products. They also allow the engineering of cells that respond to exogenous chemicals, often by changing gene expression in these cells.

Strategies to construct biosensors include RNA-based riboswitches,[5] FRET reporters,[6] and allosteric transcription factors.[7] These types of biosensors are often limited in sensitivity and can require iterative rounds of improvement to obtain ligand binding of sufficient affinity and specificity for use. An alternative approach exploits natural or computationally designed ligand-binding domains that are destabilized by mutation to be rapidly degraded in the absence of ligand.[8] Stability is rescued by binding to a small molecule ligand. Recent advances in protein engineering have yielded *de novo* designed ligand-binding domains for several small molecules, including digoxigenin,[9] fentanyl,[10] and 17a-progesterone.[11] This approach provides a path for the construction of a biosensor from a computationally designed or natural ligand-binding domain recognizing a small molecule.

Here, we report a second generation of conditionally stable eukaryotic biosensors that require both ligand binding and protein dimerization for activity. Synthetic, dimeric transcription factors have been reported to respond to isopentenyl diphosphate in yeast,[12] but their design requires a conformational switch upon ligand binding. The biosensors we describe require only that the ligand-binding domain be dimeric. The biosensors consist of two fusion proteins: a ligand-binding domain fused to a DNA-binding domain, and a ligand-binding domain fused to a transcriptional activation domain (Figure 1a). An active transcription factor is reconstituted upon small molecule binding, which stabilizes the biosensor and increases its concentration in the cell. Because each of the two ligand-binding domains binds its own ligand, this strategy also affords the opportunity to create biosensors that require two different ligands to become fully active. To test this concept, we started with the computationally designed digoxigenin-binding protein DIG10.3[9] as a homodimeric ligand-binding domain. Relative to the first-generation biosensors,[8] the background activity of our second-generation dimeric biosensors was greatly reduced because the constituents were split into different proteins.

Received: June 8, 2018
Published: September 11, 2018

DOI: 10.1021/acssynbio.8b00242
ACS Synth. Biol. 2018, 7, 2457−2467

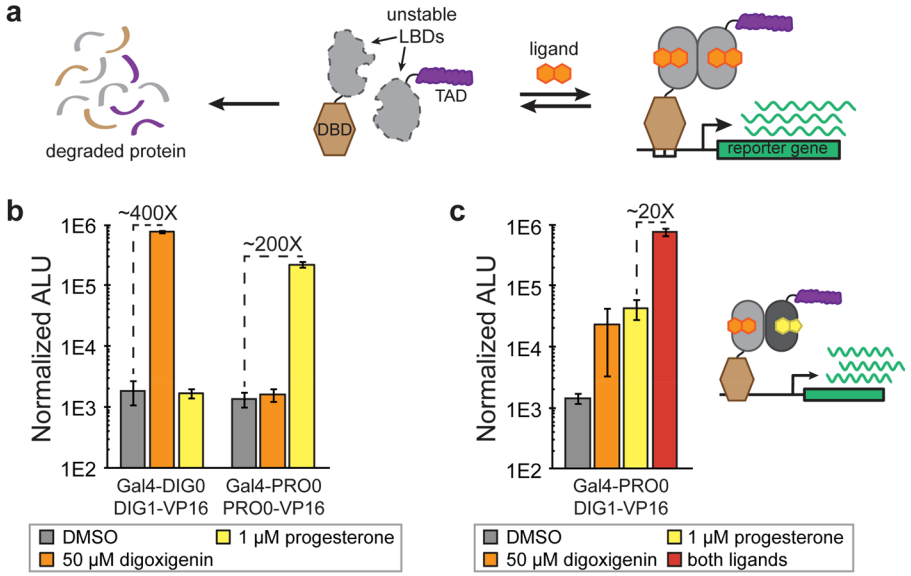

Figure 1. Validation of ligand-dependent stabilization of dimeric biosensors. (a) Cartoon illustration of the strategy to create biosensors from unstable dimeric ligand-binding domains. In the absence of ligand, the DNA-binding domain (DBD) and transcriptional activation domain (TAD) fused to ligand binding domain (LBD) monomers are degraded and inactive. Addition of ligand stabilizes both proteins, facilitating dimerization and reporter activation. (b) Activation of a luciferase reporter with a digoxigenin-dependent dimer (Gal4-DIG0 and DIG1-VP16) and a progesterone-dependent dimer (Gal4-PRO0 and PRO0-VP16). Fold activations are shown relative to no ligand (DMSO). (c) Reporter activation driven by a simple "AND"-gate using Gal4-PRO0 and DIG1-VP16. Stabilization of two different ligand-binding domains, PRO0 by progesterone and DIG1 by digoxigenin, are required for dimerization. Fold activation denotes increase in reporter expression when both ligands are present over just progesterone.

Computational redesign of the dimer interface and ligand-binding pocket allowed us to create a pair of orthogonal heterodimers that respond either to the small molecule digoxigenin or to progesterone. We further improved these biosensors using directed evolution and deep sequencing to identify mutations that favor heterodimerization and small molecule binding selectivity. Finally, we demonstrate that in combination, these approaches can result in an improved "AND"-gate and a pair of orthogonal biosensors that can selectively activate independent reporters.

RESULTS

Dimeric Biosensors Are Stabilized by Ligand Binding.

We sought to extend the functionality of ligand-stabilized biosensors through the use of homodimeric proteins. Whereas the first-generation biosensors consisted of a ligand-binding domain fused to a DNA-binding domain and transcriptional activation domain in a single polypeptide, these second-generation biosensors comprise two separate polypeptide chains: a ligand-binding domain fused to a DNA-binding domain, and a ligand-binding domain fused to an activation domain (Figure 1a). With this approach, both fusion proteins should be unstable and rapidly degrade in the absence of ligand. The ligand-binding domains become stabilized by binding to their cognate ligands, reconstituting a functional transcription factor that activates the expression of a reporter gene.

With first-generation biosensors based on the computationally designed dimeric digoxigenin-binding protein DIG10.3,[9] many of the conditionally destabilizing mutations identified by random mutagenesis and selection mapped to its homodimer interface,[8] suggesting that dimerization plays an important role in this protein's stability. We asked whether we could exploit ligand-stabilized dimerization of DIG10.3 to reconstitute an active transcription factor. We fused the DIG10.3 monomer (termed DIG0) to a Gal4 DNA-binding domain and to a VP16 activation domain and transformed a yeast strain, PF22, containing a firefly luciferase reporter gene driven by the *GAL1* promoter, with expression plasmids for both constructs. Neither protein alone activated reporter expression, but when Gal4-DIG0 and DIG0-VP16 were coexpressed, the addition of 50 μM digoxigenin induced a ~20-fold increase in luciferase activity. In comparison to the single-component sensor Gal4-DIG0-VP16, the dimeric biosensor had a wider dynamic range but generated less than 1% of the reporter activity (Supporting Figure S1a). To determine whether destabilizing mutations improved the dynamic range of the biosensor, we incorporated a mutation (E83V, creating DIG1) that improved ligand-induced stabilization in the single polypeptide biosensor context.[8] DIG1-VP16 paired with Gal4-DIG0 improved activation to ~400-fold (Figure 1b). Because E83 lies at the dimer interface, this improvement may be driven by a reduction in the self-association of DIG1-VP16, making more of it available to interact with Gal4-DIG0. A similar effect was not observed when DIG1 was fused to the Gal4 DNA-binding domain or was used in both the Gal4 and VP16 fusions (Supporting Figure S1b). Destabilization of the fusion containing the Gal4 domain may impair DNA binding, while destabilizing mutations in both sides of the dimer interface may prevent dimerization.

We next examined whether mutations to the ligand-binding pocket of DIG10.3 could make the dimers sensitive to an alternative ligand. A series of three tyrosine to phenylalanine mutations (Y34F, Y99F, Y101F, designated PRO0) in this pocket increase the affinity of DIG10.3 for progesterone, while decreasing it to digoxigenin.[9] When the PRO0 domain was individually fused to a DNA-binding domain (Gal4-PRO0) and to an activation domain (PRO0-VP16), 1 μM progester-

DOI: 10.1021/acssynbio.8b00242
ACS Synth. Biol. 2018, 7, 2457−2467

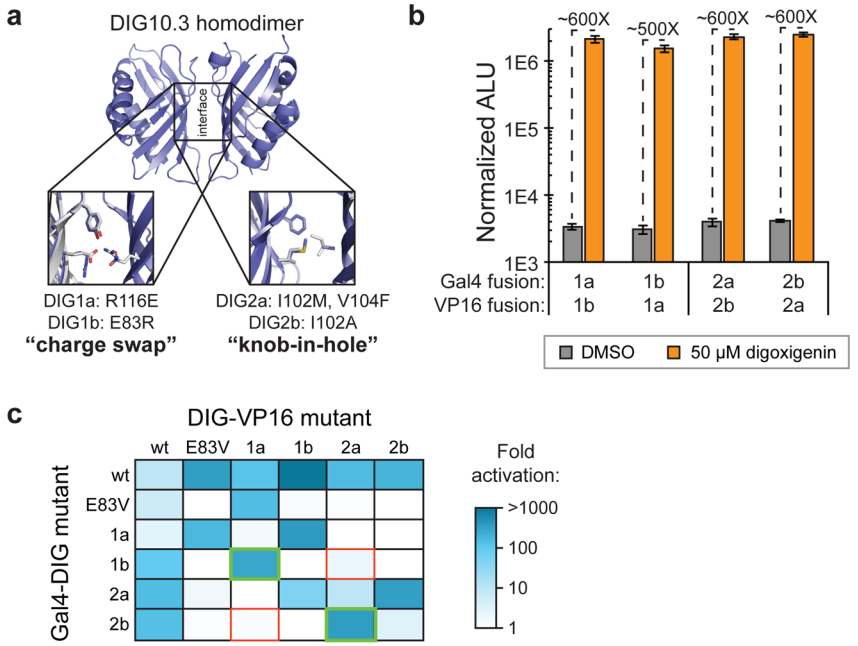

Figure 2. Engineering of dimer interfaces to create orthogonal ligand-binding domain pairs. (a) Models of the "charge swap" and "knob-in-hole" interface mutants made from the dimer structure of DIG10.3 (PDB code: 4J9A). Both the native (white) and mutant (blue) residues are shown. (b) Function of dimer interface mutants on dimeric biosensors. Each mutant pair of DNA-binding domain and activation domain fusions was tested with or without digoxigenin for activation of a luciferase reporter. (c) Heatmap of fold activation of a luciferase reporter with all possible Gal4 and VP16 fusions to DIG mutants, tested with 50 μM digoxigenin. The interaction between two heterodimer pairs chosen for further improvement are highlighted with green boxes; red boxes illustrate relevant cross reactivity.

one induced a ~200-fold increase in reporter activity (Figure 1b).

As the two ligand-binding domains must bind ligand and dimerize to function as a biosensor in this context, we considered whether a simple "AND"-gate could be generated by a combination of progesterone and digoxigenin ligand-binding domains. The mutations in PRO0 do not fall on the dimer interface, and thus this domain should be capable of dimerizing with either DIG0 or DIG1. We paired Gal4-PRO0 with DIG1-VP16 and found that luciferase activity was 20-fold greater when both ligands were present in the media than when either alone was present (Figure 1c).

Biosensor Activity Is Improved by Computational Redesign of the Ligand-Binding Domain Dimer Interface. To further improve biosensor function and provide greater control over dimerization, we redesigned the dimer interface to favor heterodimerization between the DNA-binding domain and activation domain fusions over homodimerization of two copies of the same fusion protein. We hypothesized that the dynamic range of the initial dimers was limited by nonproductive homodimers reducing the amount of functional complex. Additionally, orthogonal heterodimer interfaces would allow the use of multiple DIG-based biosensors (*e.g.*, digoxigenin-specific and progesterone-specific heterodimers) in the same cell without crosstalk between the biosensors.

Using the Rosetta software suite, we redesigned the interface of the DIG0 dimer based on a "charge swap" or "knob-in-hole" model (Figure 2a). The charge swap design introduced the mutations R116E in DIG1 (to generate DIG1a) and E83R in its partner DIG0 (to generate DIG1b). For this design, self-association should be limited by unfavorable charge−charge repulsion. The knob-in-hole design introduced a hydrophobic pocket in DIG0 (I102A, to generate DIG2b) that could be complemented with bulkier side chains in DIG1 (I102M and V104F, to generate DIG2a). For this design, homodimerization should be disfavored by steric clashes and cavities in the dimer interface. Although included in the original designs, the E83V mutation was removed after early testing revealed poor reporter activation.

Biosensors built from both designs showed a >500-fold increase in reporter activation in the presence of digoxigenin (Figure 2b). When we assessed the ability of each of the DIG10.3 mutants to interact with other variants, the heterodimer designs were largely orthogonal (Figure 2c). All of the charge swap and knob-in-hole fusion proteins potently activated reporter expression when paired with their complement and showed a weaker ability to activate reporter expression with other mutants or copies of themselves. In contrast, the unmutated interface of DIG0 paired well with any other mutant. The progesterone-binding mutations in DIG10.3 could be incorporated into both interface redesigns to create improved progesterone biosensors (Supporting Figure S2).

Selection of Mutations That Impart Improved Heterodimerization or Ligand Selectivity. Although the designed heterodimers represented a substantial improvement, we sought to use directed evolution to identify additional heterodimer pairs and increase the selectivity of the biosensors for highly similar steroid compounds. Toward this goal, we devised a selection scheme that paired a single interface mutant of the DIG-VP16 fusion with a library of random Gal4-DIG mutants generated by error-prone PCR. The library was selected for beneficial mutations using activation of a *HIS3* reporter gene in either the presence or absence of ligand. Because Gal4-DIG0 interacted with most interface mutants and these dimers responded to ligands similar to digoxigenin, we repeated the selection by varying the fixed interface mutant fused to VP16 and the ligand (Figure 3a). By comparing the

DOI: 10.1021/acssynbio.8b00242
ACS Synth. Biol. 2018, 7, 2457−2467

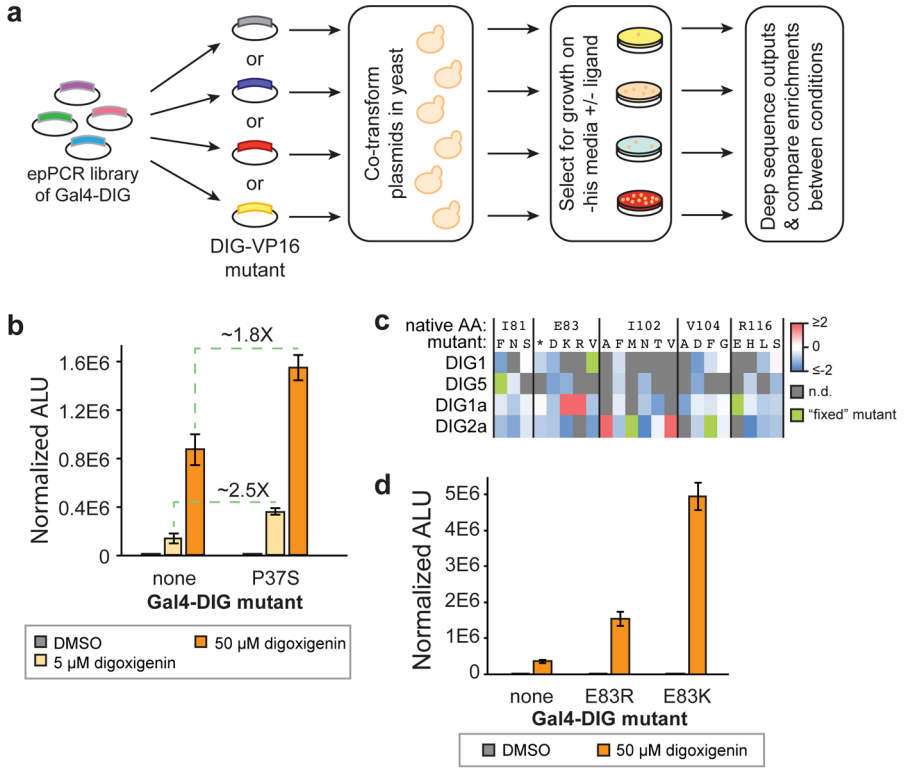

Figure 3. Selection for mutations to improve biosensor function. (a) Selection scheme used to select for mutants in Gal4-DIG. An epPCR library of DIG mutants fused to Gal4 was cotransformed with each of four "fixed" interface mutants of DIG-VP16. Transformed cells were selected for growth on media lacking histidine and in the presence or absence of a ligand. Cells were collected, deep sequenced, and mutational enrichments compared to identify effects. (b) Effect of P37S mutant of Gal4-DIG paired with DIG1-VP16 on luciferase activation with two concentrations of digoxigenin. Dotted green line represents fold increase in luciferase activity with P37S. (c) Heatmap of enrichment scores for selected interface residues with each of the four "fixed" interface mutants and 1 μM digoxigenin. Mutants with no data are shown in gray, and the "fixed" mutation used in the VP16 fusion for selection is denoted in green. (d) Effect of two Gal4-DIG mutants, E83 substituted with either lysine or arginine, when paired with DIG1a-VP16. Each was tested for the activation of a luciferase reporter with digoxigenin.

results of each selection, we could identify mutations that either: (1) generally improved dimerization and were enriched under all conditions; (2) improved the specificity of heterodimerization and were enriched only with a single fixed interface mutant; or (3) improved ligand binding selectivity and were enriched differently between ligands. This analysis was aided by the use of deep sequencing of the His+ colonies in bulk and comparison of the relative enrichment of mutations under each regime.

We tested 20 different selection conditions. Four fixed interface mutants, DIG1 (E83V), DIG5 (I81F), DIG1a (R116E), and DIG2a (I102M, V104F), fused to VP16 were each paired with the error-prone DIG10.3 library fused to the Gal4 domain. DIG1 was chosen because it dimerized well with DIG0, and DIG5, an interface mutant previously identified as destabilizing,[8] was chosen to enable selection of mutants complementary to a different part of the dimer interface. DIG1a and DIG2a represented additional interface mutations. Gal4-DIG1b and Gal4-DIG2b were doped into the library as controls, as they require two or more base pair changes and would be unlikely to arise by error-prone PCR. The transformants were plated on solid media with one of five ligand conditions: DMSO (no-ligand control); digoxigenin, at two different concentrations (1 μM or 10 μM) to assess the effect of stringency; digitoxigenin (1 μM), as a highly similar ligand that differs from digoxigenin by only a single hydroxyl group; and progesterone (1 μM), to identify more selective mutants than PRO0. Enrichment scores were calculated relative to the frequency of mutations in the unselected library.

When we averaged the enrichment scores for each position of DIG10.3 regardless of selection condition, we found that mutations to the overwhelming majority of positions in DIG10.3 were deleterious, but that a handful were enriched (Supporting Figure S3). Mapped to the structure of the DIG10.3 dimer, the enriched mutations were distributed across both the surface and the ligand-binding pocket of the protein. Several mutations were strongly selected with digoxigenin regardless of the fixed interface mutant used in the selection. Of these commonly enriched mutations, mutations to P37 were the most frequent. In the presence of digoxigenin, the addition of a P37S mutation to Gal4-DIG0 and pairing of this mutant with DIG1-VP16 roughly doubled the amount of reporter expression (Figure 3b). Because mutations to this position were so widely selected, we surmised that this benefit was the result of stabilization of the ligand-binding domain. Several other mutations enriched in all of the digoxigenin selections also demonstrated a modest increase in activation by digoxigenin (Supporting Figure S4a). The increase in activation conferred by P37S boosted the sensitivity of both of the heterodimer interfaces (Supporting Figure S4b). To confirm the hypothesis that these mutations stabilized DIG10.3, we tested them in the context of a single component biosensor (Supporting Figure S4c). In contrast with a destabilizing mutation (E83V), the addition of P37S or G95D to a Gal4-DIG0-VP16 construct more than doubled

DOI: 10.1021/acssynbio.8b00242
ACS Synth. Biol. 2018, 7, 2457−2467

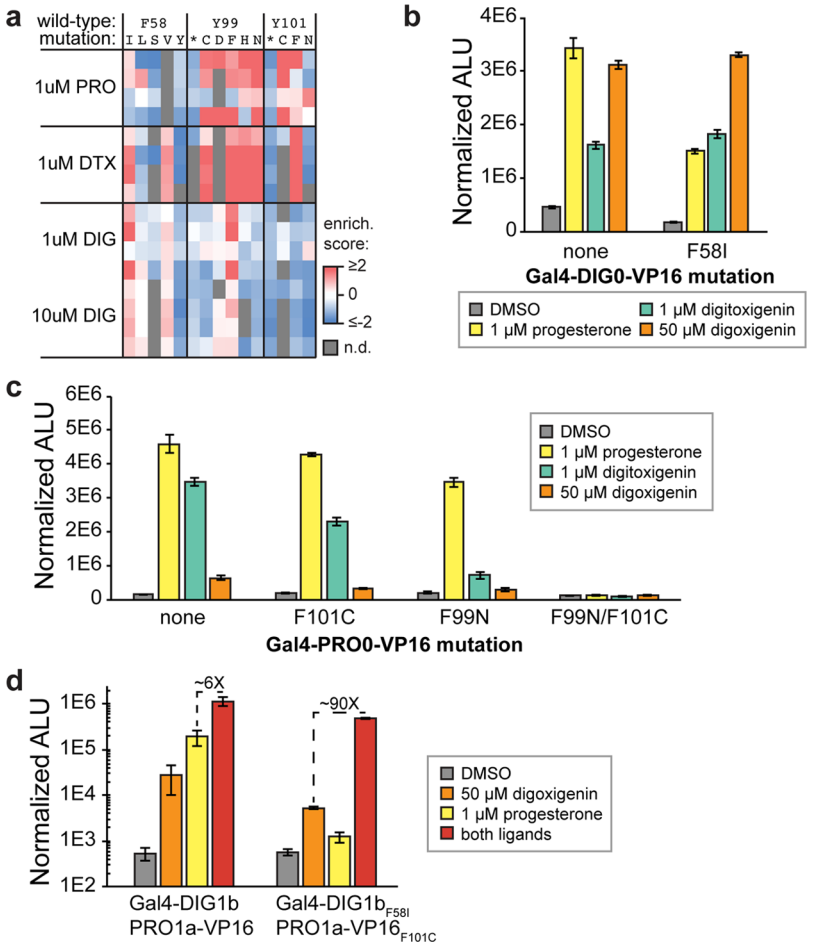

Figure 4. Identification of mutations affecting selectivity of ligand binding. (a) Heatmap of enrichment scores for mutations to three ligand-binding domain binding pocket residues that exhibited unique profiles based on the ligand used in selection. (b) Effect of a digoxigenin-selective mutation, F58I, tested in the context of a single-component, Gal4-DIG0-VP16 biosensor activating luciferase reporter expression. (c) Effect of two progesterone-selective mutants, F101C and F99N, tested in the context of a single-component, Gal4-PRO0-VP16 biosensor activating luciferase reporter expression. (d) Effect of combining heterodimerizing "charge swap" mutations and ligand-selective binding pocket mutations in both components of an "AND"-gate.

the activity of the biosensors in the absence of ligand. Because this sensor is not dependent upon dimerization, increases in its activity are likely dependent solely on stabilization by these mutations.

To identify selected mutations that might contribute to an orthogonal heterodimer interface, we compared the relative enrichment scores for positions located at the dimer interface (Figure 3c). Only in the selections using the DIG1a and DIG2a mutants did we recover uniquely enriched mutations at interface positions. Two of these enriched mutations, E83R (*i.e.*, DIG1b) and I102A (*i.e.*, DIG2b), represented complements created during the computational redesign of the heterodimers. Two similar amino acid changes, E83K and I102V respectively, were also enriched. When paired with DIG1a-VP16, both E83R and E83K mutations in Gal4-DIG performed better than without the E83 mutation (Figure 3d). All of the interface-specific mutations performed better with their fixed interface partner than did Gal4-DIG0 (Supporting Figure S5), suggesting that these mutations were under positive selective pressure.

We also identified two unexpected groups of mutations. The first consisted of mutations to the flexible linker between Gal4 and DIG (enumerated in Supporting Figure S6) that arose as the result of errors in the Gibson assembly of the libraries. When linker mutations in Gal4-DIG0 were tested with DIG1-VP16, they increased biosensor activation with digoxigenin by about 40−50% (Supporting Figure S6). This result suggests that further improvements to the biosensors might be made through linker optimization. The second group of unexpected mutations consisted of stop codons at positions 41 and 42, which were enriched with three ligands (Supporting Figure S7a). These premature stop codons might be revealing a cryptic activation domain, as mutations to acidic amino acids, which are commonly found in activation domains, also tended to be enriched in the same selections. A construct of Gal4-DIG0 truncated at position 41 was insensitive to the addition of digoxigenin and was a more potent activator of luciferase than was full-length DIG0 (Supporting Figure S7b), consistent with the truncation revealing a ligand-independent activation domain.

Mutations that conferred ligand selectivity were identified by comparing the enrichment scores among selections with digoxigenin, digitoxigenin, and progesterone. Three positions in the ligand-binding pocket of DIG10.3 had mutations that were selectively enriched (Figure 4a). F58I strongly enriched in nearly all selections with digitoxigenin or digoxigenin, but

DOI: 10.1021/acssynbio.8b00242
ACS Synth. Biol. 2018, 7, 2457−2467

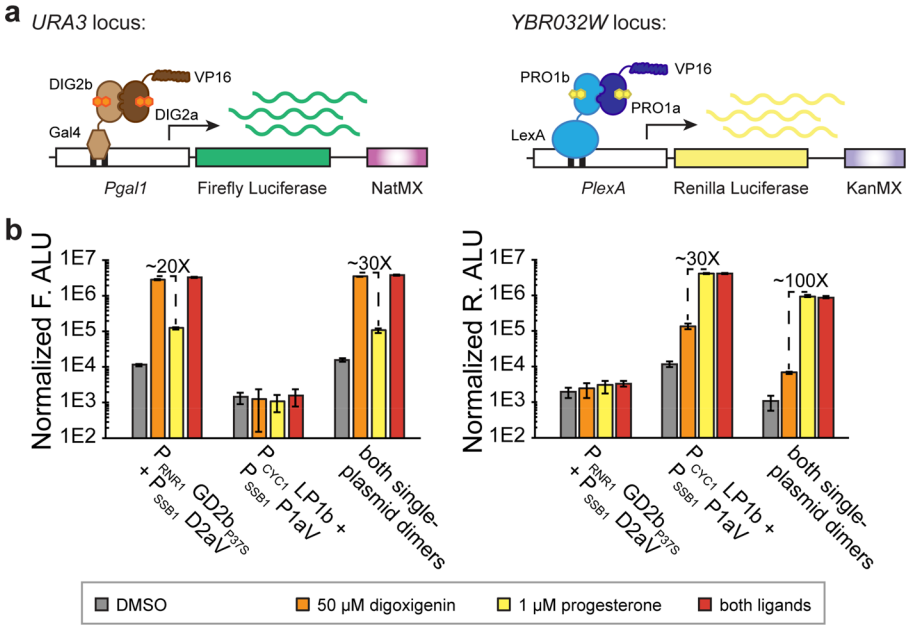

Figure 5. Use of two orthogonal biosensors to detect different ligands in the same cell. (a) Cartoon illustration of the design for orthogonal digoxigenin and progesterone biosensors. A Gal4-dependent firefly luciferase reporter is driven using the knob-in-hole heterodimeric digoxigenin biosensor. A LexA-dependent *Renilla* luciferase reporter is driven by a charge swap heterodimeric progesterone biosensor. (b) Comparison of the ability for the digoxigenin and progesterone biosensors to drive expression of a firefly luciferase (Normalized F. ALU) and a *Renilla* luciferase (Normalized R. ALU) reporter when the biosensor components are present alone *versus* when both biosensors are present in the same cell.

not with progesterone. To determine if this mutant enhanced the selectivity of DIG10.3 to bind digoxigenin and digitoxigenin over progesterone, we tested it in the context of the single component Gal4-DIG0-VP16 biosensor (Figure 4b). Activation of this F58I mutant biosensor by digoxigenin and digitoxigenin did not change, but the relative activation by progesterone was reduced significantly. Mutations to Y99 and Y101 were selectively enriched with progesterone and digitoxigenin, but not digoxigenin. Mutations at both of these positions to phenylalanine increase the relative affinity for progesterone by eliminating H-bonds to digoxigenin.[9] To test the effect of mutations that were enriched with progesterone but not digoxigenin, we assayed F101C and F99N in the context of a single component Gal4-PRO0-VP16 biosensor (Figure 4c). Although these mutations reduced the absolute activity of this biosensor with progesterone by 7% and 25%, respectively, activation by digoxigenin was reduced by more than 50% with either mutation. Despite being enriched in a background of DIG0, both mutants were less sensitive to digitoxigenin when added to PRO0. Combining both mutations in the same Gal4-PRO0-VP16 scaffold resulted in a nonfunctional biosensor, likely due to collapse of the ligand-binding pocket.

The mutations conferring improved selectivity for digoxigenin and progesterone provided an opportunity to enhance the selectivity of the dimeric biosensors. When the mutations used to create the charge swap heterodimer interface were combined with the digoxigenin and progesterone "AND"-gate pair, background activation by the single ligands increased substantially, reducing the relative activation by the addition of both ligands (Figure 4d). We surmised that the heterodimerizing mutations in this context inadvertently affected the selectivity and affinity of the ligand-binding domains for each other, making the dimers more sensitive to the presence of a single ligand. When F58I and F101C mutations were added to digoxigenin and progesterone ligand-binding domains, respectively, the functional charge swap "AND"-gate was restored.

Optimizing Biosensor Activity. We considered that the response of the dimeric biosensors might be further improved by adjusting the expression level of each component. We chose four constitutive promoters (*REV1*, *RNR1*, *SSB1*, and *TEF2*) with a range of expression levels[13,14] that spanned 2 orders of magnitude (Supporting Figure S8). Using the knob-in-hole heterodimer biosensor, we found that increasing expression of both fusion proteins yielded an increase in biosensor activity (Supporting Figure S9). However, the use of the strongest promoter, *TEF2*, to drive expression of the activation domain fusion was less effective, likely due to toxicity associated with VP16.[15] Increased expression of both components resulted in the most potent activation at lower levels of digoxigenin and a better than 1000-fold activation of luciferase activity with 50 μM ligand.

With two orthogonal dimeric pairs that respond to different ligands, it became possible to measure the activation of separate reporter genes by the addition of each ligand. We used a knob-in-hole heterodimeric digoxigenin biosensor to drive a firefly luciferase reporter and a charge swap heterodimer progesterone biosensor to drive a *Renilla* luciferase reporter (Figure 5a). For the progesterone biosensor, we replaced Gal4 with a LexA DNA-binding domain and used a modified *GAL1* promoter containing LexA binding sites to drive expression of the *Renilla* luciferase reporter. Each pair of sensor components was cloned onto a single plasmid and transformed into the dual-reporter stain PGFLR14. When single-plasmid biosensors for digoxigenin and progesterone were present in the same cell, they performed at least as well as their two plasmid counterparts (Figure 5b). The addition of mutations that enhance the selectivity of ligand binding would likely further improve the response of both sensors to the target ligand and

DOI: 10.1021/acssynbio.8b00242
ACS Synth. Biol. 2018, 7, 2457−2467

improve the separation between activation by one ligand or the other.

DISCUSSION

We show here that biosensors with a dynamic range spanning more than 3 orders of magnitude can be built from a dimeric ligand-binding domain. Compared to the previous single component transcription factors, the dimers drive expression of less reporter gene activity but have substantially improved dynamic ranges (Supporting Figure S10). Because these proteins must bind ligand, accumulate, and transduce their increased level into the activation of a reporter gene, these biosensors generally have slower kinetics than other types of biosensors, but their simplicity, ease of design, and tunability make them a desirable alternative. Biosensors based on heterodimeric ligand-binding domains may also facilitate new designs for logic-gate construction, an increasingly important utility in microbe engineering. Biosensors constituting an "AND"-gate could be used to create a checkpoint in a biosynthetic pathway that is contingent upon the presence of two metabolic precursors. "AND"-gates built from other homodimeric ligand-binding domains will require the design and engineering of a heterodimeric interface and a new ligand specificity in one of the proteins. The reliance on directed evolution to select for altered ligand-binding domains will likely restrict binding specificities to ligands that are similar to the original substrate. However, as computational protein design technologies improve, it may be possible to engineer *ab initio* a pair of dimerizing ligand-binding domains that recognize more chemically diverse molecules. Furthermore, the demonstration that these biosensors function in yeast suggests that they will do so in other eukaryotes, similar to the single fusion biosensors.[8]

The use of deep sequencing to characterize the output from the different selection conditions provides advantageous features. The prevalent selection of stabilizing mutations was unsurprising, given that such mutations are the simplest route for unstable ligand-binding domains to increase in concentration and survive the selection. Because these stabilizing mutations were so heavily enriched, it would have been difficult to identify mutations conferring ligand selectivity by sequencing individual colonies. Similarly, mutations in the linker between DIG and the DNA-binding domain were poorly represented in the library and would not have been easily identified by sequencing a handful of individual clones.

While the directed evolution scheme worked well to identify stabilizing and ligand-specific mutations, it was less successful in selecting for complementary heterodimer interfaces, *e.g.*, of DIG1 and DIG5. Conversely, the positive enrichment for the counterparts of DIG1a and DIG2a illustrates the power of selection to isolate complementary interface mutants when a counterpart is available. Saturation mutagenesis of the 10 amino acids that form the core of the dimer interface might yield more novel complementary interface pairs.

Beyond the scope of biosensors, ligand-dependent dimers provide a simple framework for modulating biological functions. For example, ligand-stabilized dimers could see use in much the same way that rapamycin and its analogues have been used to chemically regulate protein−protein interactions and intracellular protein localization.[16] With destabilized ligand-binding domains, dimerization is likely driven entirely by changes in protein concentration upon ligand binding and not by a conformational change. This feature could provide either a benefit or a liability depending on the application. As with transcription factor-based biosensors, the slower rate of activation and destabilization of the fused partners could be problematic, but they may provide a solution for systems suffering from high background activity. Wu *et al.*[17] have demonstrated the importance of these tools to medicine by using an engineered "AND"-gate to activate cancer-killing CAR T-cells. Further development of ligand stabilized dimers for a variety of synthetic biology applications will significantly expand the toolkit for controlling biological interactions.

MATERIALS AND METHODS

Yeast Methods. YPD and synthetic dropout media were prepared as in Dunham *et al.*[18] Yeast were transformed by the Gietz method.[19]

Yeast Strains. *S. cerevisiae* strains used were derived from the yeast strain PJ74. This strain was created by deleting the efflux pump *PDR5* in the yeast two-hybrid strain PJ69−4a.[20] A clean deletion of the open-reading frame was created by the 50:50 method.[21]

A firefly luciferase reporter strain was built from the *S. cerevisiae* strain PJ74. A *GAL1* promoter for firefly luciferase was cloned *via* Gibson assembly into a pUG6 plasmid,[22] adjacent to a NatMX cassette. The reporter construct and neighboring antibiotic resistance gene were amplified by PCR with primers containing 50 bp of sequence homologous to the *ura3* locus. Linear PCR product was transformed into the PJ74 strain and selected for integration on YPD agar plates containing 100 μg/mL nourseothricin. Genomic DNA for colony PCR was isolated by boiling cells from a single colony in 20 mM NaOH for 10 min, pelleting cell debris by centrifugation, and using the supernatant as template in a PCR reaction. Integration was confirmed by Sanger sequencing the genomic locus PCR amplicon. The resulting strain was named PF22.

The dual luciferase *S. cerevisiae* strain was built by adding a *Renilla* luciferase reporter to the firefly luciferase reporter strain, PF22. A construct encoding a *Renilla* luciferase ORF driven by a modified *GAL1* promoter was cloned into a pUG6 plasmid adjacent to a KanMX cassette. The modified *GAL1* promoter contained LexA DNA binding sites in place of the native Gal4 DNA binding sequences. The *Renilla* reporter construct and KanMX cassette were amplified by PCR from the plasmid using primers containing 50 bp of homology to the YBR032W locus. The purified PCR product was transformed into yeast, and transformants were plated on YPD agar with 200 μg/mL G418 and 100 μg/mL nourseothricin. Crude genomic DNA was isolated from single colonies as above and used to confirm faithful integration by PCR and Sanger sequencing. The resulting strain was name PGFLR14.

Plasmid Constructs. A list of plasmids can be found in the Supporting Information (Table S1). DIG10.3 and the destabilized mutants were cloned as DNA-binding domain and transcriptional activation domain fusions by Gibson Assembly.[23] Briefly, PCR fragments for each insert were generated using Phusion High-Fidelity DNA Polymerase (NEB, Waltham, MA) under standard PCR conditions. Amplification primers were ordered from Integrated DNA Technologies and contained 25−30 base overlaps with a neighboring insert or the plasmid backbone. Recipient vectors p415CYC and p416CYC[24] were linearized by digestion with *Bam*HI and *Sal*I (restriction enzymes from NEB, Waltham, MA) and purified by DNA Clean & Concentrator kit (Zymo

DOI: 10.1021/acssynbio.8b00242
ACS Synth. Biol. 2018, 7, 2457−2467

Research, Irvine, CA). DNA-binding domain fusions were cloned into p415CYC, and transcriptional activation domain fusions were cloned into p416CYC. Plasmids were cotransformed into *S. cerevisiae* and were plated on the synthetic dropout media lacking leucine and uracil (SD -leu -ura).

To express different levels of the biosensor components, promoters were cloned into expression plasmids by replacing the *CYC1* promoter in p415CYC and p416CYC plasmids *via* Gibson assembly. Plasmids were linearized by digestion with SacI and *Sal*I. The *TEF2* promoter was amplified from a p414TEF plasmid[24] by PCR. Promoter sequences for *REV1*, *RNR1*, and *SSB1* were amplified from genomic DNA isolated from the PJ69−4a strain. Yeast cells were lysed by boiling in 20 mM NaOH for 10 min, pelleted by centrifugation, and supernatant was used as template for PCR with Phusion polymerase (35 cycles of 98 °C for 10 s, 62 °C for 15 s, 72 °C for 45 s). Assembly reactions included both promoter and biosensor component amplicons. DNA-binding domain fusions were cloned into a p415 plasmid and transcriptional activation domain fusions were cloned into a p416 plasmid.

To create plasmids capable of expressing both biosensor components, PCR products encoding a complete transcriptional unit (*i.e.*, promoter, ORF, and terminator) were amplified and cloned by Gibson assembly. Recipient plasmids containing the coexpressed biosensor component were digested with *Sal*I. Amplification primers were designed to insert constructs such that the two ORFs were oriented in parallel, with the terminator of the first transcriptional unit next to the promoter of the second. Dimers using Gal4 as the DNA-binding domain were cloned into p415, and LexA DNA-binding domain constructs into p416.

Mutagenesis and Selection. A table of mutations tested and their functions can be found in the Supporting Information (Table S2). Mutations were introduced into the DIG domain by Gibson Assembly using mutagenic primers. Pairs of primers containing mutant codons and 30 bp of complementarity were designed as forward and reverse primers from the site of mutagenesis and used in Phusion polymerase PCR reactions with primers annealing to the 3′ and 5′ end of each gene, respectively. The resulting gene fragments containing altered codons were then reassembled in Gibson reactions into either p415CYC or p416CYC.

Random mutations were introduced to DIG10.3 with a GeneMorph II Random Mutagensis Kit (Agilent, Santa Clara, CA). Using primers immediately flanking DIG10.3, mutagenic PCR was performed according to manufacturer's protocol (95 °C 30 s, 68 °C 30 s, 72 °C 1 min, 30 cycles) using 160 ng of a p415CYC plasmid containing a Gal4-DIG0 insert as a template. The resulting PCR product was purified and cloned *via* Gibson Assembly into a p415CYC plasmid containing Gal4 and a multiple cloning site (linearized with *Hin*dIII and *Sal*I). The plasmid library was transformed into ElectroMAX DH10B cells (Thermo Fisher Scientific, Waltham, MA) *via* electroporation per manufacturer's protocol. Transformants were allowed to recover in 1 mL SOC with shaking at 37 °C for 1 h. A 1:1000 dilution of cells was plated on LB agar containing ampicillin and was found to be comprised of roughly 5×10^6 members. The library was expanded by inoculating the remainder of the transformed cells into 25 mL LB with ampicillin and grown for 18 h at 30 °C. Plasmid library was purified from culture using five Qiaprep Miniprep columns (Qiagen, Hilden, Germany). Sanger sequencing of 10 colonies revealed 2−9 bp changes per DIG, with an average mutation rate of 4 bp changes per clone.

For the selection of Gal4-DIG mutants, yeast cells were first transformed with an interface variant of DIG-VP16, followed by transformation of the mutant library. All selections were performed with the PJ74 strain; this strain also includes a *GAL1* promoter-driven *HIS3* reporter gene at the *LYS2* locus. A single plasmid encoding a DIG-VP16 interface variant was transformed into yeast and plated on SD -ura agar plates. A single colony was picked into 5 mL SD -ura liquid media and grown for 16 h at 30 °C. The cultures were back diluted to an OD_{600} = 0.1−0.2 in 50 mL and grown on a shaker at 225 rpm until the cultures doubled at least twice (5−7 h). Cells were pelleted, washed and transformed with the Gal4-DIG library on a p415CYC plasmid. The transformation was performed as five samples, with each using 500 ng of Gal4-DIG library, supplemented with 0.5 ng of plasmids encoding Gal4-DIG1b and Gal4-DIG2b, and 2×10^8 yeast. The five samples were pooled, mixed, split, and plated in equal volumes on different selective media. Each 14 cm agar plate received roughly 2×10^8 cells and was prepared from SD -ura -leu -his +1 mM 3-aminotriazole, containing either DMSO, 1 μM digoxigenin, 10 μM digoxigenin, 1 μM digitoxigenin, or 1 μM progesterone (1% final DMSO). Plates were grown for 7 days at 30 °C before all cells were collected from each plate by gentle scraping. Plasmid was isolated from the selected cells using a Zymoprep Yeast Plasmid Miniprep kit (Zymo Research, Irvine, CA). The transformation and selection was performed once for each of the five interface variants, with the 1 μM digoxigenin selections performed in triplicate.

Luciferase Assays. Single colonies of luciferase reporter strains transformed with biosensor constructs were inoculated into 200 μL of SD -leu -ura +2% glucose in a clear Costar 96-well culture plate. Replicates of three to five colonies were assayed for each transformant. Cultures were incubated at 30 °C for 6 h, and then the OD_{600} was measured with a Synergy H1 plate reader (BioTek, Winooski, VT). To capture cultures in mid log growth after overnight incubation, each culture was back-diluted to an OD_{600} = 0.1−0.15 and then serially diluted 1:3 with fresh media three times. Plates were sealed with a Breathe-Easy membrane (Sigma-Aldrich, St. Louis, MO) and incubated at 30 °C for about 16 h. The density of each culture was measured, and samples at an OD_{600} = 0.3−0.5 were used for subsequent inoculations. Each culture was then diluted into a new 96-well plate with fresh media to an OD_{600} = 0.1 in 198 μL and induced with 2 μL of 100× ligand in DMSO (1% final DMSO). Culture plates were sealed and incubated at 30 °C until the cultures had gone through 3 to 4 doublings (6−7 h).

To measure firefly luciferase activity, cultures were resuspended by pipetting, and a final OD_{600} was measured for normalizing reporter activity. 5× passive lysis buffer (125 mM Tris-phosphate, pH 7.8; 10 mM DTT; 10 mM EDTA; 50% glycerol, 10% Triton X-100, store at −20 °C) was warmed to room temperature and 25 μL was added to wells of a new 96-well plate. 100 μL of induced culture was added to each well and gently mixed by pipetting, carefully avoiding the formation of bubbles. Plates were incubated at room temperature for 20 min.

Firefly luciferase activity was measured by mixing equal volumes of lysed cultures with a firefly luciferase assay reagent (25 mM Tris, pH 7.8; 15 mM $MgSO_4$; 3 mM ATP; 2 mM EDTA; 1 mM DTT; 250 μM coenzyme A; 1 mM D-luciferin). 100 μL of lysed culture and 100 μL of firefly luciferase assay

DOI: 10.1021/acssynbio.8b00242
ACS Synth. Biol. 2018, 7, 2457−2467

reagent were gently mixed in a white 96-well LUMITRAC 200 plate (Greiner Bio-one, Kremsmünster, Austria) and incubated at room temperature for 5 min. Luciferase activity was measured on a Synergy H1 plate reader with a 1 s integration time. The activity of each sample was normalized by dividing the raw luminescence by the final OD_{600}. The average normalized luminescence and standard deviation were calculated from each set of biological replicates.

The dual luciferase assay was adapted from a published protocol[25] using a Dual-Glo Luciferase Assay (Promega, Madison, WI). The dual luciferase reporter strain was transformed with plasmids, cultured, and incubated with ligand as with the firefly luciferase assay. After cultures were treated with ligand on 96-well plates and grown for 3−4 doublings, cells were lysed by gently mixing 100 μL of culture with 25 μL of 5× Passive Lysis Buffer (Promega, Madison, WI). 50 μL of this mixture was combined with 50 μL of the Glo luciferase reagent on a white 96-well LUMITRAC plate and incubated at room temperature for 20 min. Firefly luciferase activity was measured on a Synergy H1 plate reader with a 1 s integration time. 50 μL of Stop and Glo reagent was then added to each well, and *Renilla* luciferase activity was measured after the plate was incubated at room temperature for 20 min. The final OD_{600} of each culture prior to measurement of luciferase activity was used to normalize raw luminescence, and average luciferase activities were calculated from 3 to 5 biological replicates.

Computational Redesign. The homodimer interface of computationally designed DIG binder DIG10.2 was redesigned to render it heterodimeric using the Rosetta software suite. Although all computational analysis was performed on DIG10.2 because of its higher resolution crystal structure, redesigned interfaces should translate to the higher affinity variant DIG10.3 used in this study.

DIG10.2 homodimer (PDB ID 4J8T, chains A and B) was relaxed with coordinate restraints to prepare it for design calculations.[26] A model of the conditionally unstable first-generation biosensor DIG10.2 E83V/DIG10.2 heterodimer was then generated by mutating E83 on chain A to Val and then repacking and minimizing side chains. This model was used as an input for fixed backbone interface redesign in RosettaScripts.[27] Several different design protocols were used, including Monte Carlo interface design calculations optimizing Rosetta total score,[28] greedy optimization[29] calculations optimizing interface $\Delta\Delta G$ and total score, or Monte Carlo design followed by greedy optimization of the interface core, then short-range electrostatic interactions at the interface edge, then long-range electrostatic interactions. In all calculations, native residue identity was up-weighted and the amino acids Pro, Cys, Gly, and His were disallowed if non-native. Designs having good interface metrics (Rosetta $\Delta\Delta G$, total score, Holes score,[30] and solvent-accessible surface area) were manually inspected and several were selected for further evaluation.

For each selected design, global protein docking using FastRelax refinement[31] was used to validate the designed heterodimeric interface and evaluate both corresponding undesired homodimeric interfaces. Docking was run on the distributed computing platform Rosetta@home. A successful design was one in which the desired heterodimer had a funnel-shaped docking profile,[32] in which Rosetta score is more favorable for docked configurations having low RMSD to the starting design model, and both corresponding homodimers either had nonfunnel-shaped docking profiles or had funnel-shaped docking profiles but scored poorly relative to heterodimer. Two designs, the "charge swap" design (chain A: E83V, R116E; chain B: E83R), and the "knob-in-hole" design (chain A: E83V, I102M, V104F; chain B: I102A), were experimentally evaluated.

Sequencing. To prepare samples for high throughput sequencing, amplicons encoding the selected DIG from the Gal4-DIG plasmids were generated using qPCR. PCR reactions were prepared using Phusion polymerase with 1 μL selected plasmid library, 500 nM each primer, 1× GC Phusion Buffer, 1× SYBR green, and supplemented with an additional 1 mM $MgCl_2$. A control reaction was performed using 50 ng of the naïve Gal4-DIG plasmid library. The forward and reverse amplification primers were designed to anneal 100 bp upstream and downstream of the DIG sequence, with the forward primer annealing to *GAL4* in order to reduce capture of the DIG mutant fused to VP16. Samples were run on a MiniOpticon Real-Time PCR System (Bio-Rad, Hercules, CA) and cycled (98 °C 10 s, 72 °C 30 s) until the RFU approached 0.7. The amplification of all selections was performed for 9−17 cycles before being placed on ice. PCR products were cleaned up using a DNA Clean and Concentrator Kit (Zymo Research, Irvine, CA).

Amplicons were prepared for high throughput sequencing by tagmentation. Using a Nextera DNA Library Preparation kit (Illumina, San Diego, CA), 50−100 ng of each library amplicon was fragmented according to manufacturer's protocol. Each tagmented product was purified by a DNA Clean and Concentrator Kit and used in a limited cycle PCR reaction (72 °C 3 min, 98 °C 30 s, 7 cycles: 98 °C 10 s, 63 °C 30 s, 72 °C 3 min) according to manufacturer's protocol. Uniquely indexed primers were used for each library in order to multiplex sequencing of the libraries. Products were again purified by a DNA Clean and Concentrator Kit and run on a PAGE gel; all libraries showed a smear of sizes ranging from about 150−700 bp. Two nM of each library was loaded into a NextSeq 500/550 Mid Output 300 cycle kit (Illumina, San Diego, CA), yielding a sequencing depth of about 90 000−300 000 reads per selected library.

Sequencing results from the library selections were analyzed as a pileup of amino acid changes for each position within DIG. Despite each Gal4-DIG clone containing three amino changes on average, for the analysis we made the assumption that each mutation was selected in isolation. Briefly, sequencing reads were trimmed of their Nextera adapters with Trim Galore! (https://www.bioinformatics.babraham.ac.uk/projects/trim_galore/) and overlapping forward and reverse reads were merged using PEAR.[33] Merged and unmerged reads were aligned to a reference DIG sequence using Bowtie 2.[34] Using a custom python script, each DNA sequence was translated and used to create a pileup of amino acid counts at each position within DIG. The resulting file contained a tab delimited table indicating the number of times a given amino acid was observed at each position. A complete set of scripts and detailed protocol for file analysis is available online (https://github.com/msr2009/PROTEIN_PILEUP).

Mutational enrichment scores were calculated by comparing the frequency of each mutation appearing in selection relative to its frequency in the naïve mutant library. The frequency of each mutation in the naïve Gal4-DIG library was calculated by dividing the number of counts for a given amino acid change by the sum of counts for all amino acids at that position. A

DOI: 10.1021/acssynbio.8b00242
ACS Synth. Biol. 2018, 7, 2457−2467

pseudocount of 0.5 was added to each amino acid count in order to ensure a nonzero frequency. A mutation frequency was similarly calculated from the selected libraries. An enrichment score for each mutation was calculated as the $\log_2$ of the ratio the mutant frequency under selection and the mutant frequency in the naïve library. In order to filter out low confidence enrichment scores, we required that the number of sequencing counts for any given mutation represent at least 0.1% of the total sequencing reads at a given position in DIG. No score was calculated for the native amino acid. For the selections performed in triplicate (1 μM digoxigenin), an average enrichment score was determined.

■ ASSOCIATED CONTENT

Supporting Information

The Supporting Information is available free of charge on the ACS Publications website at DOI: 10.1021/acssynbio.8b00242.

Tables S1, S2 and Figures S1−S10 (PDF)

■ AUTHOR INFORMATION

Corresponding Author

*E-mail: fields@uw.edu. Tel: (206) 616-4522.

ORCID

Benjamin W. Jester: 0000-0002-2997-7865

Present Addresses

[⊥]Biologics Group, Lumen Bioscience, Seattle, Washington 98103, United States.

[#]Department of Biology, University of Utah, Salt Lake City, Utah 84112, United States.

[¶]Amgen Discovery Research, Amgen South San Francisco, South San Francisco, California 94080, United States.

Author Contributions

B.W.J. constructed plasmids, built yeast strains, performed reporter assays and selections, and analyzed data. C.E.T. computationally designed initial heterodimer pairs. M.S.R. conceived sequencing analysis pipeline and wrote scripts. B.W.J., C.E.T., M.S.R., D.B., and, S.F. wrote the manuscript.

Notes

The authors declare no competing financial interest.

■ ACKNOWLEDGMENTS

We thank Vatsan Raman and Maitreya Dunham for comments on the manuscript. This work was supported by grant P41 GM103533 (to S.F. and D.B.). S.F. was and D.B. is an investigator of the Howard Hughes Medical Institute.

■ REFERENCES

(1) Zhang, J., Jensen, M. K., and Keasling, J. D. (2015) Development of biosensors and their application in metabolic engineering. *Curr. Opin. Chem. Biol. 28*, 1−8.

(2) Rogers, J. K., Taylor, N. D., and Church, G. M. (2016) Biosensor-based engineering of biosynthetic pathways. *Curr. Opin. Biotechnol. 42*, 84−91.

(3) Garst, A. D., Bassalo, M. C., Pines, G., Lynch, S. A., Halweg-Edwards, A. L., Liu, R., Liang, L., Wang, Z., Zeitoun, R., Alexander, W. G., and Gill, R. T. (2017) Genome-wide mapping of mutations at single-nucleotide resolution for protein, metabolic and genome engineering. *Nat. Biotechnol. 35* (1), 48−55.

(4) Wang, H. H., Isaacs, F. J., Carr, P. A., Sun, Z. Z., Xu, G., Forest, C. R., and Church, G. M. (2009) Programming cells by multiplex genome engineering and accelerated evolution. *Nature 460* (7257), 894−898.

(5) Hallberg, Z. F., Su, Y., Kitto, R. Z., and Hammond, M. C. (2017) Engineering and in vivo applications of riboswitches. *Annu. Rev. Biochem. 86*, 515−539.

(6) Zadran, S., Standley, S., Wong, K., Otiniano, E., Amighi, A., and Baudry, M. (2012) Fluorescence resonance energy transfer (FRET)-based biosensors: visualizing cellular dynamics and bioenergetics. *Appl. Microbiol. Biotechnol. 96* (4), 895−902.

(7) Dietrich, J. A., Shis, D. L., Alikhani, A., and Keasling, J. D. (2013) Transcription factor-based screens and synthetic selections for microbial small-molecule biosynthesis. *ACS Synth. Biol. 2* (1), 47−58.

(8) Feng, J., Jester, B. W., Tinberg, C. E., Mandell, D. J., Antunes, M. S., Chari, R., Morey, K. J., Rios, X., Medford, J. I., Church, G. M., Fields, S., and Baker, D. (2015) A general strategy to construct small molecule biosensors in eukaryotes. *eLife*, DOI: 10.7554/eLife.10606.

(9) Tinberg, C. E., Khare, S. D., Dou, J., Doyle, L., Nelson, J. W., Schena, A., Jankowski, W., Kalodimos, C. G., Johnsson, K., Stoddard, B. L., and Baker, D. (2013) Computational design of ligand-binding proteins with high affinity and selectivity. *Nature 501* (7466), 212−216.

(10) Bick, M. J., Greisen, P. J., Morey, K. J., Antunes, M. S., La, D., Sankaran, B., Reymond, L., Johnsson, K., Medford, J. I., and Baker, D. (2017) Computational design of environmental sensors for the potent opioid fentanyl. *eLife*, DOI: 10.7554/eLife.28909.

(11) Dou, J., Doyle, L., Jr Greisen, P., Schena, A., Park, H., Johnsson, K., Stoddard, B. L., and Baker, D. (2017) Sampling and energy evaluation challenges in ligand binding protein design. *Protein Sci. 26* (12), 2426−2437.

(12) Chou, H. H., and Keasling, J. D. (2013) Programming adaptive control to evolve increased metabolite production. *Nat. Commun. 4*, 2595.

(13) Lee, M. E., DeLoache, W. C., Cervantes, B., and Dueber, J. E. (2015) A highly characterized yeast toolkit for modular, multipart assembly. *ACS Synth. Biol. 4* (9), 975−86.

(14) Peng, B., Williams, T. C., Henry, M., Nielsen, L. K., and Vickers, C. E. (2015) Controlling heterologous gene expression in yeast cell factories on different carbon substrates and across the diauxic shift: a comparison of yeast promoter activities. *Microb. Cell Fact. 14*, 91.

(15) Gill, G., and Ptashne, M. (1988) Negative effect of the transcriptional activator GAL4. *Nature 334* (6184), 721−4.

(16) Putyrski, M., and Schultz, C. (2012) Protein translocation as a tool: The current rapamycin story. *FEBS Lett. 586* (15), 2097−105.

(17) Wu, C. Y., Roybal, K. T., Puchner, E. M., Onuffer, J., and Lim, W. A. (2015) Remote control of therapeutic T cells through a small molecule-gated chimeric receptor. *Science 350* (6258), aab4077.

(18) Dunham, M. J., Gartenberg, M. R., and Brown, G. W. (2015) *Methods in Yeast Genetics and Genomics: A CSHL Course Manual*, p 256, Cold Spring Harbor Laboratory Press, Cold Spring Harbor, NY.

(19) Gietz, R. D., and Schiestl, R. H. (2007) High-efficiency yeast transformation using the LiAc/SS carrier DNA/PEG method. *Nat. Protoc. 2* (1), 31−4.

(20) James, P., Halladay, J., and Craig, E. A. (1996) Genomic libraries and a host strain designed for highly efficient two-hybrid selection in yeast. *Genetics 144* (4), 1425−36.

(21) Horecka, J., and Davis, R. W. (2014) The 50:50 method for PCR-based seamless genome editing in yeast. *Yeast 31* (3), 103−12.

(22) Guldener, U., Heck, S., Fielder, T., Beinhauer, J., and Hegemann, J. H. (1996) A new efficient gene disruption cassette for repeated use in budding yeast. *Nucleic Acids Res. 24* (13), 2519−24.

(23) Gibson, D. G., Young, L., Chuang, R. Y., Venter, J. C., Hutchison, C. A., 3rd, and Smith, H. O. (2009) Enzymatic assembly of DNA molecules up to several hundred kilobases. *Nat. Methods 6* (5), 343−5.

(24) Mumberg, D., Muller, R., and Funk, M. (1995) Yeast vectors for the controlled expression of heterologous proteins in different genetic backgrounds. *Gene 156* (1), 119−22.

(25) Merritt, G. H., Naemi, W. R., Mugnier, P., Webb, H. M., Tuite, M. F., and von der Haar, T. (2010) Decoding accuracy in eRF1 mutants and its correlation with pleiotropic quantitative traits in yeast. *Nucleic Acids Res. 38* (16), 5479−92.
(26) Nivon, L. G., Moretti, R., and Baker, D. (2013) A Pareto-optimal refinement method for protein design scaffolds. *PLoS One 8* (4), e59004.
(27) Fleishman, S. J., Leaver-Fay, A., Corn, J. E., Strauch, E. M., Khare, S. D., Koga, N., Ashworth, J., Murphy, P., Richter, F., Lemmon, G., Meiler, J., and Baker, D. (2011) RosettaScripts: a scripting language interface to the Rosetta macromolecular modeling suite. *PLoS One 6* (6), e20161.
(28) Fleishman, S. J., Whitehead, T. A., Ekiert, D. C., Dreyfus, C., Corn, J. E., Strauch, E. M., Wilson, I. A., and Baker, D. (2011) Computational design of proteins targeting the conserved stem region of influenza hemagglutinin. *Science 332* (6031), 816−21.
(29) Nivon, L. G., Bjelic, S., King, C., and Baker, D. (2014) Automating human intuition for protein design. *Proteins: Struct., Funct., Genet. 82* (5), 858−66.
(30) Sheffler, W., and Baker, D. (2010) RosettaHoles2: a volumetric packing measure for protein structure refinement and validation. *Protein Sci. 19* (10), 1991−5.
(31) Berger, S., Procko, E., Margineantu, D., Lee, E. F., Shen, B. W., Zelter, A., Silva, D. A., Chawla, K., Herold, M. J., Garnier, J. M., Johnson, R., MacCoss, M. J., Lessene, G., Davis, T. N., Stayton, P. S., Stoddard, B. L., Fairlie, W. D., Hockenbery, D. M., and Baker, D. (2016) Computationally designed high specificity inhibitors delineate the roles of BCL2 family proteins in cancer. *eLife*, DOI: 10.7554/eLife.20352.
(32) Chaudhury, S., Berrondo, M., Weitzner, B. D., Muthu, P., Bergman, H., and Gray, J. J. (2011) Benchmarking and analysis of protein docking performance in Rosetta v3.2. *PLoS One 6* (8), e22477.
(33) Zhang, J., Kobert, K., Flouri, T., and Stamatakis, A. (2014) PEAR: a fast and accurate Illumina Paired-End reAd mergeR. *Bioinformatics 30* (5), 614−20.
(34) Langmead, B., and Salzberg, S. L. (2012) Fast gapped-read alignment with Bowtie 2. *Nat. Methods 9* (4), 357−9.

DOI: 10.1021/acssynbio.8b00242
ACS Synth. Biol. 2018, 7, 2457−2467